Water Research 233 (2023) 119780

Contents lists available at ScienceDirect

Water Research

journal homepage: www.elsevier.com/locate/watres

On the importance of temporal floc size statistics and yield strength for population balance equation flocculation model

Jorge A. Penaloza-Giraldo [a,*], Tian-Jian Hsu [a], Andrew J. Manning [a,b,f], Leiping Ye [c], Bernhard Vowinckel [d,e], Eckart Meiburg [e]

[a] Department of Civil and Environmental Engineering, Center for Applied Coastal Research, University of Delaware, Newark, DE 19716, United States
[b] HR Wallingford Ltd, Coasts and Oceans Group, Wallingford OX10 8BA, United Kingdom
[c] School of Marine Sciences, Sun Yat-sen University, Zhuhai, Guangdong 519082, China
[d] Leichtweiß-Institute for Hydraulic Engineering and Water Resources, Technische Universität Braunschweig, Braunschweig, Lower Saxony 38106, Germany
[e] Department of Mechanical Engineering, UC Santa Barbara, Santa Barbara, CA 93106, United States
[f] School of Biological and Marine Sciences, University of Plymouth, Plymouth, Devon, PL4 8AA, United Kingdom

ARTICLE INFO

Keywords:
Flocculation
Population balance equation
Cohesive sediment
Yield strength

ABSTRACT

Many aquatic environments contain cohesive sediments that flocculate and create flocs with a wide range of sizes. The Population Balance Equation (PBE) flocculation model is designed to predict the time-dependent floc size distribution and should be more complete than models based on median floc size. However, a PBE flocculation model includes many empirical parameters to represent important physical, chemical, and biological processes. We report a systematic investigation of key model parameters of the open-source PBE-based size class flocculation model FLOCMOD (Verney, Lafite, Claude Brun-Cottan and Le Hir, 2011) using the measured temporal floc size statistics reported by Keyvani and Strom (2014) at a constant turbulent shear rate S. Results show that the median floc size d_{50}, in terms of both the equilibrium floc size and the initial floc growth, is insufficient to constrain the model parameters. A comprehensive error analysis shows that the model is capable of predicting three floc size statistics d_{16}, d_{50} and d_{84}, which also reveals a clear trend that the best calibrated fragmentation rate (inverse of floc yield strength) is proportional to the floc size statistics considered. Motivated by this finding, the importance of floc yield strength is demonstrated in the predicted temporal evolution of floc size by modeling the floc yield strength as microflocs and macroflocs giving two corresponding fragmentation rates. The model shows a significantly improved agreement in matching the measured floc size statistics.

1. Introduction

Unlike non-cohesive sediment such as sand, cohesive sediments exhibit a unique physical process called flocculation that causes individual particles to stick together when two or more particles collide. Through flocculation, the role of cohesive sediments in aquatic environments has a crucial impact on the ecosystem. When particulate concentrations in the water column are high, aquatic organisms face severe consequences due to the absence of photosynthesis, low levels of dissolved oxygen and depletion of energy sources (Jones et al., 2012; Vaz et al., 2019). Simultaneously, cohesive sediments exert a fundamental control on the fate of nutrients and organic matter and, hence, alter the water quality (Asmala et al., 2022). Furthermore, low-density hydrophobic substances such as oil droplets can be deposited on the seafloor due to flocculation with suspended particulate matters (Daly et al., 2016; Ye et al., 2021). Therefore, studying flocculation dynamics of cohesive sediment is an important and thriving research subject in aquatic science and engineering.

Flocculation is defined by two main processes that coexist simultaneously, aggregation, and fragmentation (breakup). Aggregation may take place when cations from dissolved salt in water create surface bridging around clay particles and decrease their repulsion force (Sutherland et al., 2015). Moreover, cohesion between particles can be significantly increased by bio-cohesion such as extra-cellular polymeric substance (EPS) (Malpezzi et al., 2013; Passow and Alldredge, 1995). For energetic aquatic systems, flow turbulence is considered as the dominant mechanism driving particle collision, which is quantified by the turbulent shear rate (Mhashhash et al., 2018; Spicer and Pratsinis,

* Corresponding author.
E-mail address: japg@udel.edu (J.A. Penaloza-Giraldo).

https://doi.org/10.1016/j.watres.2023.119780
Received 21 October 2022; Received in revised form 12 February 2023; Accepted 20 February 2023
Available online 24 February 2023
0043-1354/

1996). This is directly responsible for floc formation and the growth of different floc sizes and their respective densities (porosity; e.g. Lawrence et al., 2022).

Simultaneous with the aggregation process, the flocs can experience a fragmentation (breakup) that decreases their size due to turbulent shear in energetic environments. Flocs can maintain their complex structures up to a specific size because of the floc strength maintained by inter-particle bonds (Bache et al., 1999; Jarvis et al., 2005). The flocs become more fragile as their size increases, and flocs can be broken up when a shear or tensile stress overcomes the floc strength (Yeung and Pelton, 1996). Unfortunately, quantifying the floc strength is not trivial due to difficulties in direct measurement, and a variety of factors, such as mineral types, zeta-potential, floc structures, turbulent shear must be quantified (Jarvis et al., 2005; Sharp et al., 2006; Spencer et al., 2022). Thus, most of the numerical models use a constant value of the floc strength for simplicity (Maggi et al., 2007; Verney et al., 2011; Winterwerp, 1998). In this study, we investigate the limitation of the constant floc yield strength assumption and begin to explore an alternative with satisfactory results.

The single floc size statistic method (Winterwerp, 1998) is usually implemented to track the temporal evolution of the median floc size d_{50}. Although this method has been used in many studies (Kuprenas et al., 2018; Son and Hsu, 2009), it is not designed to represent the complex floc size distribution. On the other hand, the most detailed method is to simulate flocculation using a grain-resolved approach since it tracks all the individual cohesive particles in a fully resolving turbulence field (Vowinckel et al., 2019). This allows to compute the floc strength and the fractal dimension by analyzing the bonds between the primary particles and the floc size/shape. The challenge lies in its limitation to represent practical flocculation problems due to its high computational cost. The middle-ground approaches are to model the floc size distributions. The distribution-based model (Maerz and Wirtz, 2009) requires the assumption of a fixed distribution, which constrains the bimodal floc behaviors observed in aquatic systems (Lee et al., 2011; Manning and Dyer, 2007; Soulsby et al., 2013). This limitation can be overcome by solving Population Balance Equations (PBE) that calculate the number of flocs for each given size class while maintaining the mass balance (Verney et al., 2011; Mietta et al., 2011). Many studies focus on calibrating multiple model parameters in the PBE-based size-class flocculation model using the equilibrium or temporal evolution of median floc size d_{50} (Jeldres et al., 2015; Shen et al., 2018; Zhang et al., 2019), or floc size distribution at the equilibrium state (Coufort et al., 2007). A systematic PBE model calibration was carried out by Mietta et al. (2011) using temporal evolution of the median floc size d_{50} and the equilibrium floc size distribution for a wide variety of compositions (clay type, salt type and different salinity). Importantly, using the temporal evolution of d_{50}, this study showed an inverse proportionality between the collisional efficiency and the zeta-potential. However, it is unclear whether the optimal model parameters can be well constrained by these limited physical quantities.

Motivated by the increasing popularity of PBE flocculation models for cohesive sediment transport applications (Liu et al., 2019; Sherwood et al., 2018), the main goal of this study is to advance the understanding of several key model parameters of the PBE flocculation model and how they determine the resulting temporal evolution of floc size statistics driven by a constant turbulent shear rate. Motivated by the earlier studies on PBE modeling (Verney et al., 2011; Mietta et al., 2011) and floc yield strength (e.g., Jarvis et al., 2005), the specific objectives of this study are to (1) confirm whether the median floc size statistics d_{50}, in terms of both the equilibrium floc size and the initial floc growth, is sufficient to constrain the model parameters, (2) investigate if the model parameters can be better constrained by using the temporal evolution of different floc size statistics, and (3) understand the importance of floc yield strength in the predicted floc size statistics. The remainder of the paper is organized as follows. Section 2 provides a description of the PBE-based size-class flocculation model and the laboratory data used. Section 3 focuses on extensive model investigations and error analyses for predicting the measured data. Section 4 is dedicated to investigating the floc yield strength in the flocculation model and Section 5 concludes this study.

2. Flocculation model description and configuration

2.1. PBE-based size-class flocculation model

The PBE-based size-class flocculation model FLOCMOD (Verney et al., 2011) is adopted to study the physics of flocculation. The model is based on solving PBEs, namely the temporal evolution of the number concentration of each floc size class (i.e., number-based distribution) in a homogeneous isotropic turbulent flow, and it can be written as

$$\frac{dn_k}{dt} = G_{aggr}(k) + G_{break\_shear}(k) - L_{aggr}(k) - L_{break\_shear}(k) \tag{1}$$

where n (unit m^{-3}) is the number concentration (number of flocs per unit volume) of the k^{th} floc size class, t is time (s), G and L with subscripts represent the gain and loss of class k flocs due to aggregation (subscript *aggr*) or breakup induced by turbulent shear stress (subscript *break_shear*). In estuarine and coastal environments, flows are generally energetic, and the model assumes that the turbulent shear is the dominant mechanism driving flocculation. Other aggregation mechanisms resulting from Brownian motion and differential settling are neglected (Maggi et al., 2007). For the low sediment concentration considered in this study, we also neglect the gain and loss of class k due to collision-induced breakup. The gain G_{aggr} and loss L_{aggr} by aggregation are written as

$$G_{aggr}(k) = \frac{1}{2}\sum_{i+j=k} \alpha A(i,j) n_i n_j \tag{2}$$

$$L_{aggr}(k) = \sum_{i=1}^{N} \alpha A(i,k) n_i n_k \tag{3}$$

where A is the two-body collision probability function for spherical particles and α is the collisional efficiency, which parameterizes the sticking properties of flocs and other physical processes not modeled by A (e.g., preferential accumulation that encourages collision or the effect of porosity). This parameter α is assumed constant for the calibration process following Verney et al (2011). Since we assume that the main driving force for flocculation is the turbulent shear, the two-body collision probability function depends on the turbulent shear rate S and the diameters of two colliding flocs, written as

$$A(i,j) = \frac{1}{6} S\left(d_i + d_j\right)^3 \tag{4}$$

where d_i and d_j are the spherical equivalent diameters of two colliding flocs of discrete classes i and j.

The gain G_{break_shear} and loss L_{break_shear} by breakup driven by turbulent shear stress S are defined as

$$G_{break\_shear}(k) = \sum_{i=k+1} FDBS_{ki} B_i n_i \tag{5}$$

$$L_{break\_shear}(k) = B_k n_k \tag{6}$$

where *FDBS* is the distribution function of fragmented flocs representing the gain of daughter flocs from larger floc size classes. Following Verney et al., (2011), we specify the binary distribution assuming that the mass of a floc after breakup is divided in half. The rate at which flocs break due to the turbulent shear rate S is given by the function B, and it is defined as

$$B_i = \beta S^{3/2} d_i \left(\frac{d_i - d_p}{d_p} \right)^{3-f_d} \tag{7}$$

where d_p is the primary particle diameter, f_d is the fractal dimension (Kranenburg, 1994) for equivalent spherical diameter, and β is the fragmentation rate. The fragmentation rate is in fact a dimensional quantity ($s^{1/2} \cdot m^{-1}$) and it is written as (Maggi et al., 2007; Winterwerp, 1998)

$$\beta = E \left(\frac{\mu}{F_y} \right)^{\frac{1}{2}} \tag{8}$$

where μ ($Pa \cdot s$) is the dynamic viscosity of water, E is an empirical (dimensionless) parameter and F_y (N) is the floc yield strength. Although β is a dimensional quantity, it is assumed to be an empirical constant in Verney et al. (2011). This inevitably presumes that the floc yield strength F_y is a constant, which is consistent with the fractal approach (Kranenburg, 1994). Because the direct measurement of floc yield strength is difficult, the assumption of a constant F_y is commonly adopted by many other studies (e.g., Maggi et al., 2007; Wang et al., 2013).

Verney et al. (2011) have pointed out that both the collisional efficiency α and fragmentation rate β are sensitive model parameters that need to be calibrated first with a given cohesive sediment sample. Although the fractal dimension f_d has been estimated from many laboratory and field experiments (e.g., Manning et al., 2010) to be around 2 to 2.5 and there may be a floc size dependency (Khelifa and Hill, 2006; Maggi, 2007) such that larger flocs are more porous and the interparticle bonds are smaller; assuming a constant fractal dimension within a given flocculation experiment remains to be the most practical approach. To successfully calibrate these three empirical parameters concurrently for a given experiment, sufficient information from the measured data is necessary, and a proper calibration strategy may also benefit from a more thorough examination of the governing equations to be solved.

By substituting equations (2) to (6) into the equation (1), the resulting number concentration equation of each floc size class k is written as

$$\frac{dn_k}{dt} = \frac{1}{2} \sum_{i+j=k} \alpha \frac{1}{6} S (d_i + d_j)^3 n_i n_j + \sum_{i=k+1} FDBS_{ki} \beta S^{3/2} d_i \left(\frac{d_i - d_p}{d_p} \right)^{3-f_d} n_i \\ - \sum_{i=1}^{N} \alpha \frac{1}{6} S (d_i + d_j)^3 n_i n_k - \beta S^{3/2} d_k \left(\frac{d_k - d_p}{d_p} \right)^{3-f_d} n_k \tag{9}$$

During the initial stage of the flocculation (i.e., floc growth stage), the breakup terms can be neglected (the second and fourth term on the right-hand-side (RHS) of equation (9)) since flocs must grow from small flocs or primary particles and the aggregation terms (first and third terms on the RHS) are dominant. This means that a model calibration focusing on the initial flow growth stage allows us to mainly calibrate α (Mietta et al., 2011). However, beyond the initial floc growth stage, the breakup terms must become important because there must be a balance between aggregation and breakup so that an equilibrium can be reached. Following the analysis presented in Winterwerp (1998), mean equilibrium floc size must depend on the ratio of $r = \alpha / \beta$ and fractal dimension f_d. Therefore, both the equilibrium stage and the initial floc growth stage should be considered for a complete calibration procedure.

Further insights into equilibrium floc size distribution can be gained by setting $dn_k/dt = 0$ in equation (9) which renders an expression for number concentration of each floc size class as

$$n_k = \frac{\left[\frac{1}{12} \frac{r}{S^{1/2}} \sum_{i+j=k} (d_i + d_j)^3 n_i n_j + \sum_{i=k+1} FDBS_{ki} d_i \left(\frac{d_i - d_p}{d_p} \right)^{3-f_d} n_i \right]}{\left[\frac{1}{6} \frac{r}{S^{1/2}} \sum_{i=1}^{N} (d_i + d_j)^3 n_i + d_k \left(\frac{d_k - d_p}{d_p} \right)^{3-f_d} \right]} \tag{10}$$

In addition to $r = \alpha / \beta$ and f_d, the breakup distributions functions $FDBS_{ki}$ also control the floc size distribution and must be considered in the calibration. However, the physical evidence of floc breakup distribution function is limited, and most studies assume a binary breakup. Nevertheless, if we focus on very large floc fractions (e.g., macroflocs), their gain due to breakup (G_{break_shear}) and loss due to aggregation (L_{aggr}) can be assumed insignificant compared with the smaller size fraction. Therefore, equation (10) for the very large floc size fraction can be reduced approximately to

$$n_k = \frac{\left[\frac{1}{12} \frac{r}{S^{1/2}} \sum_{i+j=k} (d_i + d_j)^3 n_i n_j \right]}{\left[d_k \left(\frac{d_k - d_p}{d_p} \right)^{3-f_d} \right]} \tag{11}$$

where the breakup distribution function $FDBS_{ki}$ disappears. Comparing the modeled large floc size statistic with measured data allows calibrating the parameters α, β and f_d with minimum impact of $FDBS_{ki}$. On the other hand, the breakup distribution function $FDBS_{ki}$ must be important for fine floc fractions. Thus, calibrating different size class statistics is valuable, particularly for the coarse floc fraction to avoid uncertainty in $FDBS_{ki}$.

Additional analysis of equation (9) is performed to compare the aggregation and breakup timescales. Following Winterwerp (1998), we estimate the initial floc growth timescale using the aggregation term in the equation (9) and it is written as

$$T_{agg} = \frac{1}{\alpha S \phi_{f,k}} \tag{12}$$

where $\phi_{f,k}$ is the volumetric concentration of floc of size class k. The above expression shows that the collisional efficiency α controls the initial floc growth timescale, and an appropriate calibration process for α should be based on the initial growth time series (Mietta et al., 2011). On the other hand, at the later stage of the floc growth before reaching equilibrium, the floc breakup must play an important role to counteract aggregation. We can examine the breakup timescale as inversely proportional to β and $S^{3/2}$ as

$$T_{brk} \sim \frac{1}{\beta S^{3/2}} \tag{13}$$

For example, to expedite floc growth at the later transient stage, the breakup timescale must be decreased by increasing β (i.e., increase the effect of breakup), which is equivalent to reducing floc yield strength. This point will be revisited in Section 4.

2.2. Experimental data

Keyvani and Strom (2014) report a flocculation experiment in a mixing tank using a mixture of kaolinite and montmorillonite clay. The flocculation experiment was performed for approximately 1800 *min* by using a total sediment mass concentration of $C = 0.05\ kg/m^3$ and a homogeneous turbulence shear rate S of 35 s^{-1}. Hence, the study neglects more complex transport mechanism such as differential advection and settling. Although homogeneous turbulence is highly idealized, it allows a comprehensive calibration of model parameters before the model can be used in conditions with increasing complexity. In addition to the measured median floc diameter d_{50} at equilibrium, Keyvani and Strom (2014) also provide measured temporal evolutions of three different floc size statistics, d_{16}, d_{50} and d_{84} (see Fig. 1) by computing a series of image ensemble every 1 to 5 minute depending on the phase (growth or equilibrium). This comprehensive dataset is selected to calibrate key empirical model parameters in the PBE-based size-class flocculation model of Verney et al. (2011). We simulate three important aspects in the measured time series, the equilibrium state ($t \geq 700$ *min* in Fig. 1), the floc growth stage ($t \leq 200$ *min* in Fig. 1), and the entire time series. In particular, matching the modeled initial floc growth stage with measured data allows us to evaluate the model's ability to predict

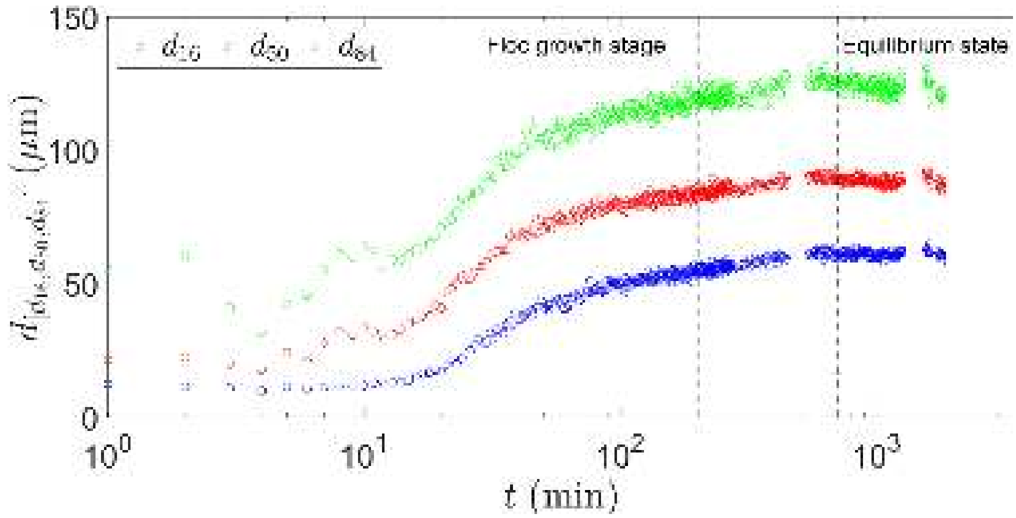

Fig. 1. Measured data reported by Keyvani and Strom (2014) for the temporal evolution of three floc size statistics (d_{16}, d_{50} and d_{84}). The analysis presented here further divides the time series into the initial floc growth stage (initial flocculation rate, $t \leq 200$ min) and the equilibrium state ($t \geq 700$ min).

the flocculation rate, which has been used by other studies to further quantify the stickiness of flocs (Ye et al., 2021) and to calibrate collisional efficiency (Mietta et al., 2011). The abundance of measured data allows a deeper calibration of the model parameters.

2.3. Flocculation model configuration

Following Keyvani and Strom (2014), the total mass concentration and turbulent shear rate from the experiment are prescribed accordingly in the flocculation model. The minimum floc size diameter is established as $d_{\min} = 4\ \mu m$, which corresponds to the diameter of the primary particle typically used for flocculation modeling (Winterwerp, 1998). The maximum floc size is specified to be $d_{\max} = 300\ \mu m$ to ensure the modeled distribution is sufficiently wide and to avoid fluctuations in the distributed mass concentration at the equilibrium state (see Figure S1 in supplementary material). Since Keyvani and Strom (2014) did not discuss the initial floc size distribution, our exploratory numerical experiments show that using a log-normal distribution represents the experimental data better than punctual distribution especially at the early stage of floc growth (see Figure S2 in supplementary material).

Following Verney et al. (2011), an explicit (Euler) time integrator is implemented to solve the PBEs (Equation 1) with an initial time step size equal to 1 s, which is also specified as the maximum allowable time step size throughout the integration. If this value is insufficient to preserve the total sediment mass within a threshold, the time step is decreased by half and the cycle is recomputed until the mass conservation criterion is satisfied. The flocculation model of Verney et al. (2011) requires the use of many classes to discretize the floc diameter distribution. Therefore, establishing the minimum number needed for an accurate numerical solution of the size distribution is an important step. The evaluation is carried out with different numbers of size class N_c to discretize the distribution. Verney et al. (2011) recommended $N_c = 15$ to be sufficient based on calibrating the median floc size d_{50} at the equilibrium state. However, our results suggest that even at $N_c = 25$, the low resolution negatively affects the predicted temporal evolution and, hence, the flocculation rate (see the first 80 minutes of floc growth in Fig. 2a) for fine, median, and coarse fractions. Another issue is the pronounced step-like feature during the floc growth when N_c is small. Careful examination of the model results indicates that the step-like feature is due to coarse numerical discretization of the floc size distribution, but not the time step, (the absence of certain size classes causes a jump in modeled size statistics during floc growth). A converged solution can be obtained when $N_c \geq 75$. In Fig. 2b, we evaluate this convergence by using the Root-Mean-Square-Error *RMSEc* from the target solution using $N_c = 200$. Large errors are observed when $N_c = 15$ especially for the coarse fraction ($RMSEc_{d_{84}} > 40\ \mu m$). By increasing the N_c to 25 and 50, the errors decrease significantly. Our additional numerical experiments suggest that the convergence evaluation is not sensitive to a variation of model parameter of α, β and f_d within a reasonable range. In the rest of the paper, we use $N_c = 75$ to maintain an affordable computational time

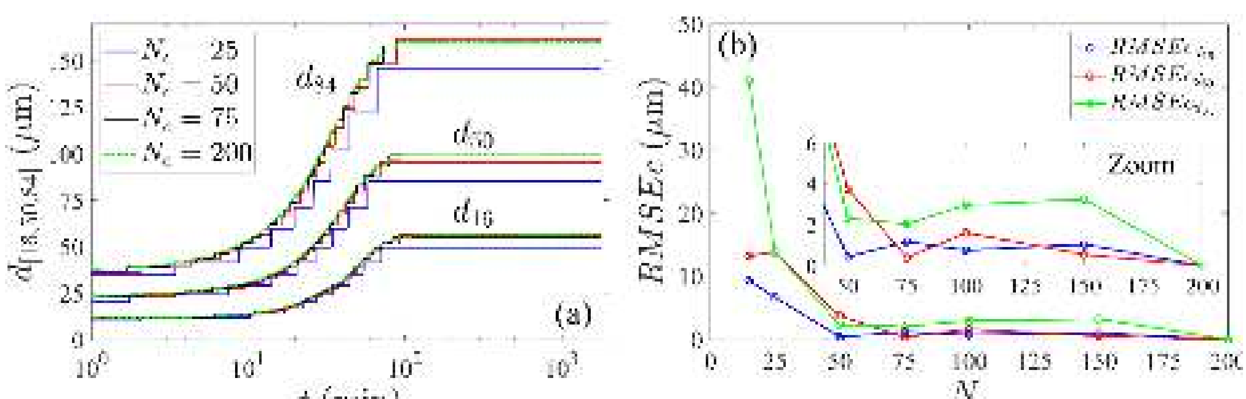

Fig. 2. Convergence analysis for different N_c. (a) Temporal evolution of floc size statistics $d_{[16,\ 50,84]}$ with different number of classes N_c. (b) Root-Mean-Square-Error *RMSEc* for different N_c.

(around 20 minutes per simulation in workstation) with $RMSEc_{d_{[16,50,84]}} \leq 0.5 \sim 3\ \mu m$.

3. Results

Motivated by the previous study of Verney et al. (2011), we concurrently calibrate α and β to match measured data and evaluate if the resulting fractal dimension f_d falls within the expected range. 6, 400 simulations were carried out using $\alpha = 5\ \times 10^{-2} \sim\ 80\ \times 10^{-2}$ with an interval of $5\ \times 10^{-2}$, and $\beta = 2\ \times 10^{-3} \sim\ 80\ \times 10^{-3}$ with an interval of $2\ \times 10^{-3}$ for ten different fractal dimension values in the range of 1.7 to 2.9. All simulations use a computational time of 1800 *min*. Using the measured data (Keyvani and Strom, 2014) as reference, three different RMSE are computed to evaluate the model performance at the equilibrium state *RMSEeq* ($t \geq 700$ *min*), the growth stage of flocculation *RMSEfr* ($t \leq 200$ *min*), and the entire flocculation time series *RMSEfp* for the tri-temporal floc size statistics d_{16}, d_{50} and d_{84} (see Figures S3~S5 in the Supplemental Material). In Section 3.1 and 3.2, the search for the optimized parameters α, β and f_d is carried out exclusively to match measured d_{50} by these three criteria, namely, minimizing the errors at the equilibrium state $\min(RMSEeq_{d_{50}})$, at the initial growth stage of flocculation $\min(RMSEfr_{d_{50}})$, and for the entire time series $\min(RMSEfp_{d_{50}})$. In Section 3.3, two more criteria are imposed (objective functions) by matching measured fine and coarse fractions, i.e., $\min(RMSEfp_{d_{16}})$ and $\min(RMSEfp_{d_{84}})$.

3.1. Temporal evolution of median floc size d_{50}

The median floc size d_{50} is the most widely reported quantity in laboratory experiments and field observations. We analyze the model's capability to represent the flocculation process using exclusively d_{50} with constraints of the parameters α, β and f_d. Moreover, since many studies only report the median floc size in the equilibrium state, it is important to investigate if the model can reproduce the entire measured time series by solely calibrating model parameters using the equilibrium median floc size.

Using the measured data from Keyvani and Strom (2014) as reference, the RSME at the equilibrium state $RMSEeq_{d_{50}}$ ($t \geq 700$ *min*) is calculated for the 6,400 simulations and results are summarized in Fig. 3 for all combinations of the parameters α, β for any given f_d. Each interaction between these parameters is examined in a simulation with the error magnitudes demarcated by a hot colormap. The dark-red color represents excellent agreement with measured d_{50} in the equilibrium state. Importantly, all the fractal dimensions ($f_d = 1.7 \sim 2.9$) show multiple choices of α and β that are in very good agreement ($RMSEeq_{d_{50}} = 1.72\ \mu m$, the finite value of 1.72 μm reflects the variabilities in the measured data) with the measured d_{50} at the equilibrium state. Clearly, low error values cluster around a line with a constant

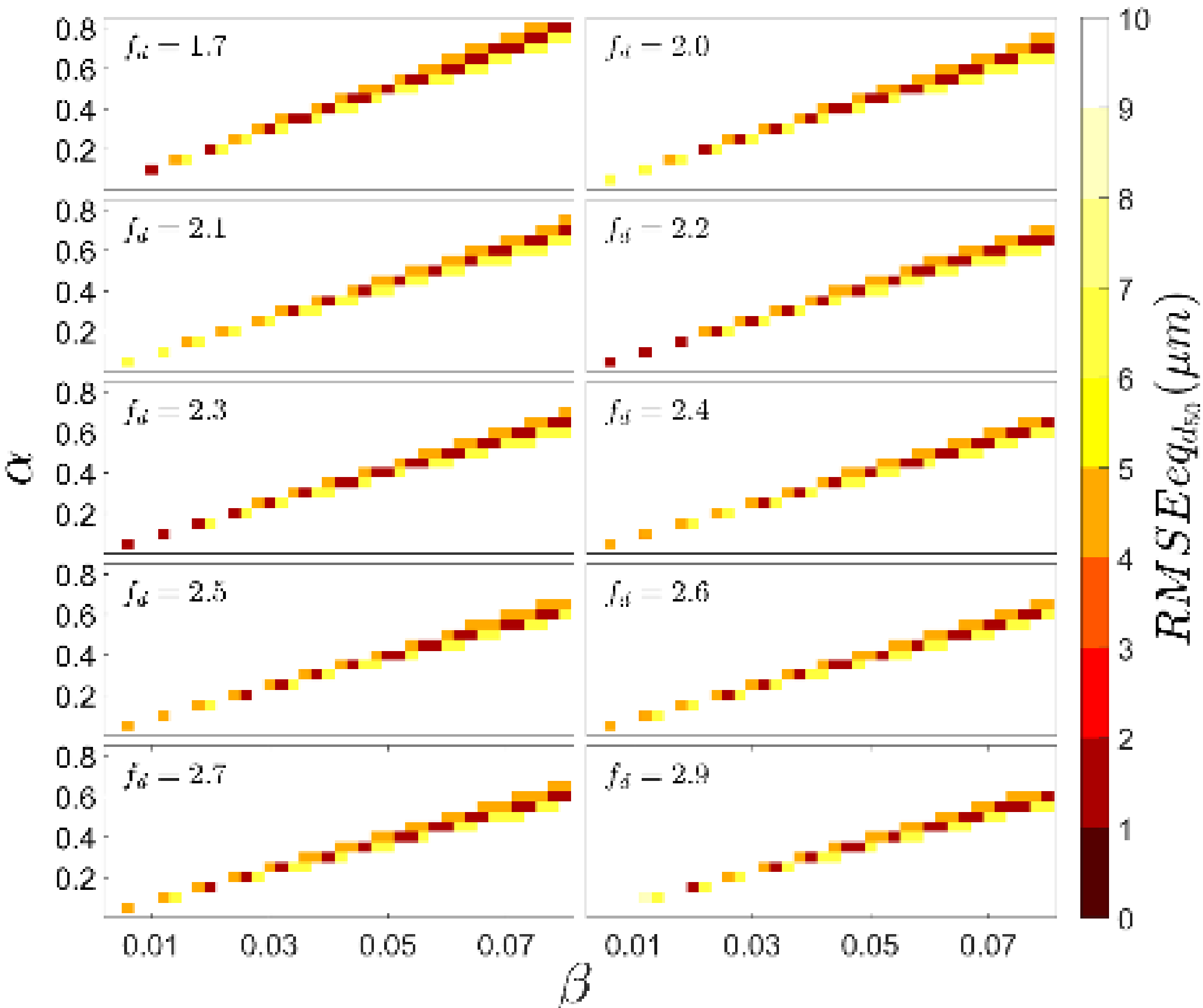

Fig. 3. Root-Mean-Square-Error matrix for the median floc size d_{50} in the equilibrium state for different combinations of collisional efficiency α and fragmentation rate β at fractal dimension f_d from 1.7 to 2.9.